

REVIEW

Open Access



Analysis of cooperative jamming against pulse compression radar based on CFAR

Xiang Liu*  and Dongsheng Li

Abstract

One important issue in radar jamming is the effect of inaccuracies in the radar position, which leads to a number of false targets entering the reference window of the constant false alarm ratio (CFAR) detector to reduce greatly. In this paper, two cooperative jamming methods specifically developed for a pulse compression radar with a CFAR detector are proposed with the aim of increasing the number of false targets when there is uncertainty regarding the radar position. First, several key parameters of the false targets are derived based on the principle of CFAR detection. Then, the principle, which takes advantage of two cooperative jamming methods to achieve a distribution of multiple false targets, is described. Finally, the influence of radar's uncertain position on the two cooperative jamming methods is simulated and analyzed in detail. The simulation result shows that both jamming methods can effectively reduce the radar's recognition rate, but there is a large difference when different interference modes are used by jammers. The obtained conclusion provides guidance for the practical application of cooperative jamming against pulse compression radar.

Keywords: Constant false alarm rate detection, Cooperative jamming, Pulse compression radar, Radar uncertain position

1 Introduction

In radar detection, the returned signals from radar targets are often buried in nonstationary noise, clutter, and interference. Classical detection using a fixed threshold is no longer applicable due to the nonstationary nature of the background. To obtain a predictable and consistent performance, a radar system designer usually prefers a constant false alarm rate (CFAR) [1].

Two of the major CFAR detectors are the cell averaging (CA) CFAR and the orderly statistics (OS) CFAR [2]. The first detector (CA-CFAR) is the optimum CFAR processor in a homogeneous background, but it has severely degraded performance on the clutter edge and with interfering targets' echoes [3, 4]. Hence, the OS-CFAR has been proposed to alleviate the problem caused by a nonhomogeneous background [5]. The OS-CFAR trades a small loss in detection performance relative to the CA-CFAR in ideal conditions for much less performance degradation in non-ideal conditions; this trade has been simulated by Blake [6].

A detector, especially an OS-CFAR detector, has a very strong anti-interference capability, which causes significant issues for the interferer [1, 2]. Methods for deceiving pulse compression radar equipped with a CFAR detector have received increased attention in the recent past. The impact of interrupted-sampling repeater jamming on a radar using constant false alarm rate detection was analyzed in [7]. Specifically, the detection costs of CA-CFAR, OS-CFAR, and censored mean level detector (CMLD) CFAR detectors for active decoy using jamming were analyzed. To evaluate the radar detection performance in a situation with multiple false targets, Fang et al. [8] analyzed typical CFAR detectors in an interfering target background. Unfortunately, specialized jamming methods against CFAR detectors were not proposed in [7] or [8]. To solve this problem, a multiple-false-target jamming method against a linear frequency modulation (LFM) pulse compression radar with a mean level (ML) CFAR detector was proposed in [9, 10]. Most of the mentioned studies have focused on CA-CFAR detectors. There are currently few specialized jamming techniques for OS-CFAR detectors, which are designed for multiple false targets.

* Correspondence: liuxiang0802@126.com

College of Electronic Engineering, National University of Defense Technology, No. 460, Huang Shan Road, Shu Shan District, Hefei, Anhui, People's Republic of China

Radar jamming technology is in high demand because it is indispensable for counteracting the pulse compression gain of the victim radars. As a result, the radar parameters and the environment are often idealized during the process of jamming research. In fact, it is inevitable that there is an uncertainty in the radar position, which is obtained through electronic reconnaissance. The number of false targets entering the reference window of the CFAR detector is greatly reduced when there are inaccuracies in the radar position. At this time, the significant disadvantage of jamming generated by a single jammer is revealed. Existing ECMs are mostly classified into barrage jamming and deception jamming. Noise barrage jamming is not sensitive to the radar's uncertain position, but it is difficult for noise barrage jamming generated by a single jammer to obtain an effective pulse compression gain in the pulse compression radar [11]. Additionally, it is necessary to add the number of the jammers to increase the power of noise barrage jamming. Coherent deception jamming based on DREFM can achieve a high pulse compression gain [12], but it is sensitive to the radar's uncertain position. According to the law of conservation of energy, simply increasing the number of false targets with a single jammer will cause a decrease in the jamming power. To increase the number of false targets, cooperative jamming generated by multiple jammers is required.

Cooperative jamming is a cooperative countermeasure technology. It was developed based on UAV airborne jammers, missiles, or balloon-borne jammers. Since 2000, the Defense Advanced Research Projects Agency (DARPA) has successively proposed low-cost UAV clustering technologies (LOCUST), such as Wolfpack electronic warfare technology [13], the Gremlins programme [14], and offensive swarm-enabled tactics (OFFSET) [15]. The key technologies, such as an unmanned cluster self-organizing network, formation control, and launch recycling, have been demonstrated by DARPA, the US Air Force Research Laboratory (AFRL), and the US Department of Defense (DoD) [16], thus providing technological support for cooperative jamming. Currently, research on cooperative jamming is mainly focused on two aspects: multi-UAV phantom tracks and multi-jammer power partitioning. Some initial concepts for generating coherent radar phantom tracks using cooperating vehicles were introduced in [17]. Subsequently, the flyable ranges for an ECAV for the same class of phantom tracks were developed by Purvis et al. [18] and generalized bounds were presented for initial conditions. Recently, an optimal ECAV and coherent phantom track mission were designed considering high dimensionality and geometric constraints [19]. To solve the power partitioning problem for cooperative electronic jamming, a simulated annealing algorithm (SA)

[20], two-person zero-sum game theory (TPZS) [21], and improved genetic algorithms (IGA) [22] have been proposed to distribute jamming power to radars. A coherent phantom track is another active area of cooperative jamming research [23, 24].

Based on the previous analysis, most cooperative jamming studies focus on the resource allocation problem, but there is currently little specialized analysis for cooperative jamming against pulse compression radar based on CFAR. Considering the fact that there is a radar uncertain position in practice, we propose two cooperative jamming methods specifically for pulse compression radar with a CFAR detector. Subsequently, the key parameters, such as the number and the power of the false targets, are derived based on the detection principle of the CFAR. In the simulation section, the performances of different interference modes in the CA-CFAR and OS-CFAR are analyzed when there is uncertainty in the radar position. Then, the required power or number of the cooperative jamming is calculated.

The contributions of the paper can be summarized as:

- (1) We propose two cooperative jamming methods specifically for the pulse compression radar with a CFAR detector.
- (2) We consider the effect of radar position inaccuracies on radar jamming and calculate the required power or amount of cooperative jamming with the presence of a radar uncertain position.
- (3) Performances of cooperative jamming with different interference modes in CFAR, especially in OS-CFAR, are analyzed. The obtained conclusion provides guidance for the practical application of cooperative jamming against pulse compression radar.

The remainder of the paper is organized as follows. First, the model of the CFAR detection is deduced based on cooperative jamming. In Section 2, according to the definition and classification of cooperative jamming, two methods of generating cooperative jamming are proposed. In Section 3, a theoretical analysis and computer simulation justify the methods' validity and efficiency. Finally, Section 4 concludes the paper.

2 Model description

2.1 Analysis of OS-CFAR processors

Radar uses different CFAR detectors depending on the detection environment. The CA-CFAR processor has a maximum detection probability in a homogeneous background. It exhibits severe performance degradation in the presence of an interfering target. OS-CFAR is relatively immune to the presence of interfering targets among the reference cells [6]. The various modifications of CA-CFAR and OS-CFAR detectors considered in this

paper are shown in Fig. 1. Two reference windows (Y_1, Y_2) are formed from the sum of $R/2$ cell outputs on the leading and lagging side of the test cell. The output of the selection logic is the sum of the two window outputs in the CA-CFAR, and the k th largest output in the OS-CFAR.

In a general CFAR detection scheme, the square-law detected video range samples are sent serially into a shift register of length $R + 1$ as shown in Fig. 1. The statistic Z , which is proportional to the estimate of noise or the interference target power, is formed by processing the contents of R reference cells surrounding the test cell containing D . A target is declared to be present if D exceeds the threshold αZ . Here, α is a constant scale factor used to achieve a desired constant false alarm probability for a given window of size R when the total background noise is homogeneous.

From [1, 2], the false alarm probabilities of the CA-CFAR and OS-CFAR in a homogeneous background can be written as

$$P_{FA,CA} = (1 + \alpha)^{-R} \tag{1}$$

$$\ln(P_{FA,OS}) = f(\alpha, R, K) - f(0, R, K) \tag{2}$$

The variable K is the rank of the cell whose input is selected to determine the threshold of the OS-CFAR. According to [25], the following function is defined

$$f(\alpha, R, K) = \ln\left(\frac{(R-K+\alpha)!}{(R+\alpha)!}\right) \approx (\alpha + R - K + 1/2) \ln(\alpha + R - K) - (\alpha + R + 1/2) \ln(\alpha + R) + \frac{K}{12(\alpha + R - K)(\alpha + R)} + K \tag{3}$$

Similarly, the detection probabilities of the CA-CFAR and OS-CFAR as a function of the signal-to-noise ratio (SNR) can be written as

$$P_{D,CA} = (1 + \alpha_D)^{-R} \tag{4}$$

$$\ln(P_{D,OS}) = f(\alpha_D, R, K) - f(0, R, K) \tag{5}$$

where

$$\alpha_D = \alpha / (1 + SNR) \tag{6}$$

Assuming there are r units in the reference cells occupied by the interference targets, the presence of interfering target returns among the reference cells raises the threshold and the detection of the primary target becomes seriously degraded. According to (1) and (2), the new false alarm probabilities of the CA-CFAR and OS-CFAR in a multiple-false-target background can be written as

$$P_{J,FA,CA} = (1 + \alpha)^{-r} \left(1 + \frac{\alpha}{1 + \chi_j}\right)^{r-R} \tag{7}$$

$$\ln(P_{J,FA,OS}) = f\left(\alpha\left(1 + \chi_{jk}\right), R, K\right) - f(0, R, K) \tag{8}$$

where χ_j is the average interference-to-noise ratio (INR) of the false targets among the CA-CFAR reference cells and χ_{jk} is the INR of the k th largest output of the OS-CFAR. Similarly, according to (4) and (5), the new detection probabilities of the CA-CFAR and OS-CFAR are obtained by replacing α with α_D . Thus

$$P_{J,D,CA} = \left(1 + \alpha_D\left(1 + \chi_j\right)\right)^{-r} (1 + \alpha_D)^{r-R} \tag{9}$$

$$\ln(P_{J,D,OS}) = f\left(\alpha_D\left(1 + \chi_{jk}\right), R, K\right) - f(0, R, K) \tag{10}$$

2.2 The jamming parameters setting requirements

In a homogeneous environment, only the noise inside the radar receiver is considered. According to the radar equation, the SNR of the target can be calculated as

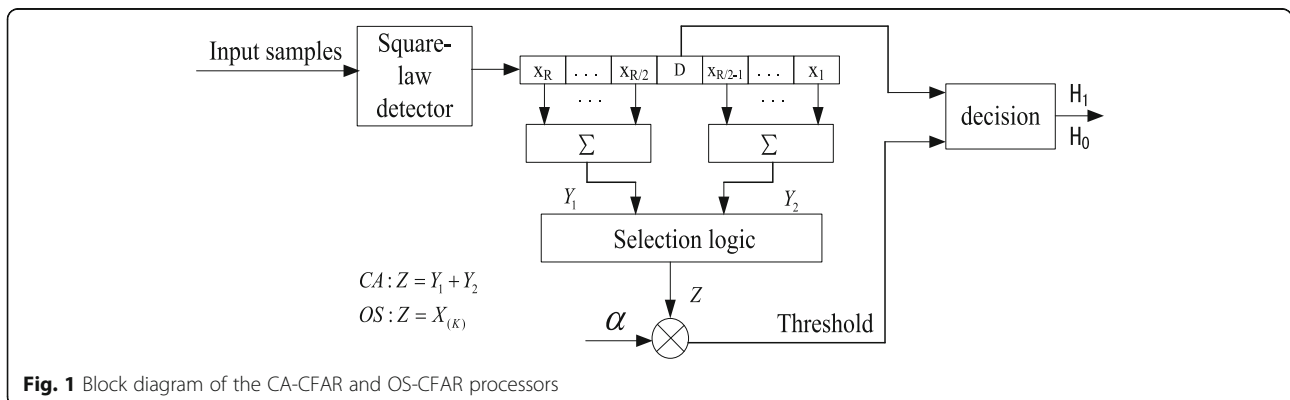


Fig. 1 Block diagram of the CA-CFAR and OS-CFAR processors

$$SNR = \frac{P_t G_t G_r \lambda^2 \sigma D}{(4\pi)^3 R_t^4 k T_0 B_r F L_t} \tag{11}$$

where P_t is the radar’s transmission power, G_t and G_r are the radar antenna transmission and reception gains, respectively, λ is the radar signal wavelength, σ is the target RCS, D is the pulse compression ratio, R_t is the distance from the radar to the target, k is the Boltzmann constant, T_0 is the effective noise temperature, B_r and F are the receiver bandwidth and noise figures, respectively, and L_t is the radar feeders and atmospheric losses.

It is assumed that the jammers are independent of one another and that the interference signal powers are linearly superimposed at the radar receiver. According to the jamming equation in [22], the total INR can be calculated as

$$\chi_j = \sum_{i=1}^n \frac{P_{ji} G_{ji} G_{ri}(\theta_i) \lambda^2 D_{ji}}{(4\pi)^2 R_{ji}^2 k T_0 B_r F \gamma_{ji} L_{ji}} \tag{12}$$

where P_{ji} is the i th jammer transmission power, R_{ji} is the distance from the radar to the i th jammer, γ_{ji} is the polarization mismatch factor, and L_{ji} contains jammer feeders and atmospheric losses, etc., G_{ji} is the jammer antenna transmission gain, $G_{ri}(\theta_i)$ is the gain of the radar antenna on the i th jammer, and $G_{ri}(\theta_i)$ can be calculated by the following empirical formula

$$G_r(\theta_i) = \begin{cases} G_r(\theta_i) & (0 \leq |\theta_i| < \frac{\theta_{i0.5}}{2}) \\ K_1 \left(\frac{\theta_{i0.5}}{\theta_i}\right) \cdot G_r & (\frac{\theta_{i0.5}}{2} \leq |\theta_i| < \frac{\pi}{2}) \\ K_1 \left(\frac{2\theta_{i0.5}}{\pi}\right) \cdot G_r & (\frac{\pi}{2} \leq |\theta_i| < \pi) \end{cases} \tag{13}$$

where $\theta_{i0.5}$ is the radar half-power beam width and θ_i is the angle between the i th jammer and the line from the radar to the target. K_1 is a constant, which for high-gain antennas generally has a value from 0.07 to 0.10, and for low-gain antennas the value ranges from 0.04 to 0.06.

For the given false probability and detector parameters in (6)–(10), in order to reduce the radar detection probability to a pre-set value, the INR in (12) must meet certain requirements. It can be seen from (12) that the INR is mainly affected by the number of jammers, the transmitted power, and the matched gain of the interference signals, which can be achieved by selecting different interference coordination methods and interference modes.

According to the above concepts, the steps for setting the jammers’ parameters can be derived as follows:

- Step 1. Calculate the SNR of the target echo via (11) with the assumption that the radar parameters have been detected.
- Step 2. Calculate the INR under two detection modes via (6)–(10). In this step, it is assumed that the false alarm probability, the pre-set minimum detection probability, and the detector parameters are known.
- Step 3. Calculate the number of jammers, the transmitted power, and the matched gain of the interference signals in (12) by selecting different interference coordination methods and interference modes.

Figure 2 shows the block diagram of the above steps.

3 Cooperative jamming

Cooperative jamming is an efficient interference method for the target, in which multiple jammers are organized to work together in a certain pattern [26]. According to the different situations in a cooperative jamming implementation strategy, cooperative jamming can be divided into power-cooperative jamming and time-cooperative jamming.

Cooperative jamming is generally generated by small-scale jammers, which have limited power. There will be a radar uncertain position in the actual interference process. From the previous analysis, jamming against pulse compression radar with a single jammer has a significant disadvantage when there is radar position inaccuracy. In

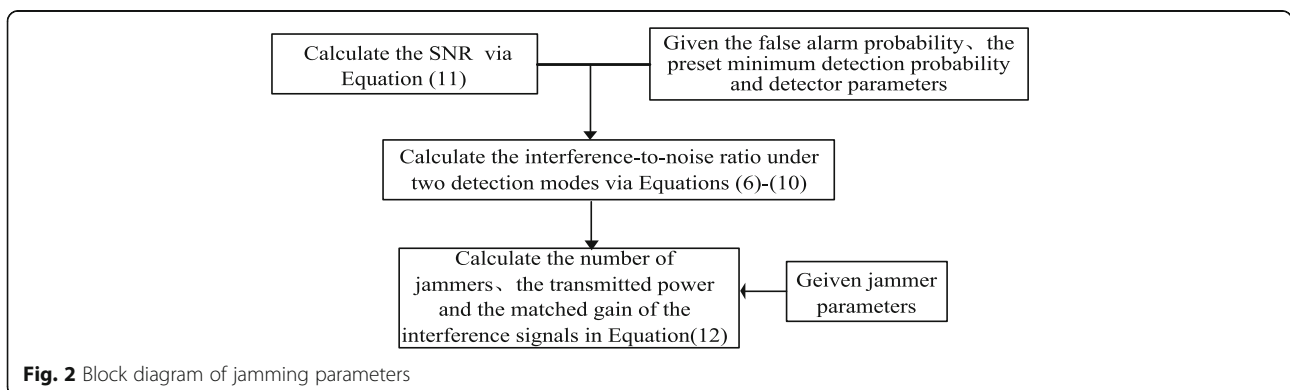


Fig. 2 Block diagram of jamming parameters

this case, multiple jammers are required to implement barrage jamming on the same area to increase the barrage power. The kind of cooperative interference mentioned above is called power-cooperative jamming.

Modern radars generally have characteristics such as a multi-beam, wide frequency band, and high power, with antennas that can simultaneously scan large areas of airspace. Therefore, multiple jammers need to consider the time-cooperative jamming problem in adjacent areas. The multi-directional false targets generated by electronic combat air vehicles in different airspaces and at different azimuths make it difficult for radar systems to detect real targets in the cover corridor. From the above analysis, it can be concluded that the goal of time-cooperative jamming is to increase the total interference time to increase the interference barrage area during the entire interference process.

3.1 Power-cooperative jamming

Power-cooperative jamming generated by two jammers is shown in Fig. 3, when there is a radar uncertain position.

It can be seen from (12) that χ_j is mainly affected by the jammers' transmitter power and the matched gain of the jamming signals. It is generally believed that the transmitter power is fixed after the type of jammer to be used is determined. The following content mainly analyzes the matched gains of different interference modes after being matched by radar and considers the influence of different interference modes on the radar detection probability when a position error is involved.

The pulse compression gains of common interference modes are not analyzed in this paper because of limited space. For a detailed analysis, one can refer to [22, 27]. This article only lists the results in Table 1.

Referring to Table 1, noise frequency modulation jamming generally has a large barrage range for radar. In the presence of a radar uncertain position, the interference signal can also cover the reference window of the radar's CFAR detector, but the interference signal power

Table 1 The pulse compression gains of different interference modes

Jamming modes	Pulse compression gains
Noise frequency modulation jamming	$T_r/T_n + T$
Smart noise convolution jamming	$T_n + T/T_n + 1/B$
Interrupted-sampling and periodic repeater jamming	$\eta^2 BT$

Note: T is the pulse duration, T_n is the noise duration, B is the bandwidth, and η is the duty ratio of the sampling signal

is small. In this situation, increasing the number of jammers in the radar main lobe increases the interference power, so the probability of radar detection is reduced.

For smart noise convolution jamming, the longer the noise duration is, the greater the barrage range for the radar and the smaller the pulse compression gain. Similar to noise frequency modulation jamming, smart noise convolution jamming is insensitive to radar uncertain position. To maintain the balance between noise power and barrage range, we can increase the INR by increasing the number of jammers when the noise duration is large. When the noise duration is small, the position of the jammer can be adjusted to compensate for the lack of interference barrage range.

Due to the time-frequency coupling of LFM signals, interrupted-sampling and periodic repeater jamming can be regarded as types of interference that are sent back to the radar with different time delays. The number of primary false targets generated by interrupted-sampling and periodic repeater jamming is not only related to the pulse width but also related to the sampling duration and the transmitting duration. The following presents a detailed analysis of this issue.

Assume that the number of false targets generated by the jammer is M , the interval of the false targets is the same Δd , and the barrage range of interference is $\Delta D = (M - 1)\Delta d$. Assume that the radar uncertain position is

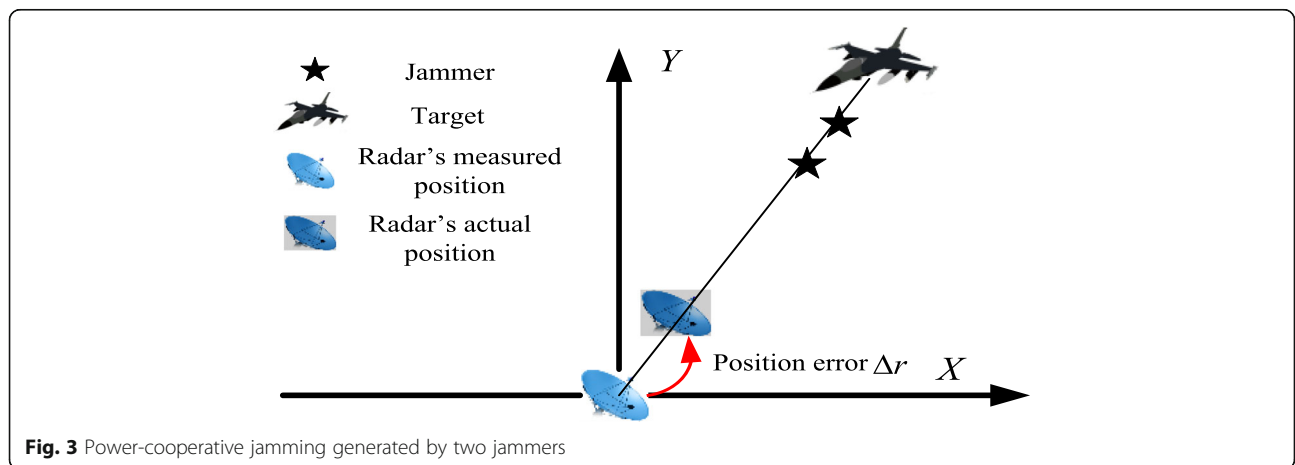


Fig. 3 Power-cooperative jamming generated by two jammers

Δr , and the length of the reference cell is L . From the analysis in Section 2.1, we know that a CA-CFAR detector is sensitive to the number of false targets. The change in the number of false targets in the reference window will have a significant impact on the CA-CFAR detector. According to [6], the performance of the OS-CFAR detector degrades rapidly when the number of false targets in the reference cells satisfies $M \geq R - K$. The impact of the false targets on the two detectors is analyzed with the change in the barrage range ΔD when there is a radar uncertain position.

Case 1: $\Delta D \geq (R + 1)L + \Delta r$

In this case, the radar uncertain position does not affect the number of false targets in the reference window and does not affect the detection result of the two detectors.

Case 2: $(R + 1)L \leq \Delta D \leq (R + 1)L + \Delta r$

When $\Delta r \leq \Delta D - (R + 1)L$, the radar uncertain position does not affect the number of false targets in the reference window, which has no effect on the detection result of the two detectors.

As the radar uncertain position increases to $\Delta D - (R + 1)L < \Delta r \leq \Delta D - (R + 1)L + (M - 1 - (R - K))\Delta d$, the number of false targets in the reference window decreases by $\text{ceil}(\frac{\Delta r - \Delta D + (R + 1)L}{\Delta d} + 1)$. $\text{ceil}(\bullet)$ means rounding up to the nearest integer. In this case, only the detection probability of the CA-CFAR detector will decrease.

When $\Delta r > \Delta D - (R + 1)L + (M - 1 - (R - K))\Delta d$, the number of false targets in the reference window is less than $R - K$, and the detection probability of the two detectors will decrease.

Case 3: $\Delta D \leq (R + 1)L$

When $\Delta r \leq (R + 1)L - \Delta D$, the position error does not affect the number of false targets in the reference window, which has no effect on the detection result of the two detectors.

As the radar uncertain position increases to $(R + 1)L - \Delta D < \Delta r \leq (R + 1)L - \Delta D + (M - 1 - (R - K))\Delta d$, the

number of false targets in the reference window will decrease. In this case, only the detection probability of the CA-CFAR detector will decrease.

As $\Delta r > (R + 1)L - \Delta D + (M - 1 - (R - K))\Delta d$, the number of false targets in the reference window is less than $R - K$, and the detection probability of the two detectors will decrease.

For case 2 and case 3, the position of one of the jammers can be used as a reference, and the number of false targets in the reference window can be increased by adjusting the distance of the other jammers. The maximum coverage of the false targets generated by multiple jammers is

$$\Delta D_{\max} = \sum_{i=1}^n M_i \Delta d_i \tag{14}$$

3.2 Time-cooperative jamming

It is difficult for a jammer to deceive radar in real time due to the fast scanning speed of the radar antenna. To increase the distribution range of the false targets in the airspace during radar scanning, the airspace position of the jammers should be reasonably arranged, and the total interference time can be increased to achieve the purpose of time-cooperative jamming.

Time-cooperative jamming can be divided into time-synchronized cooperative jamming and time-circulating cooperative jamming according to the different interference durations of each jammer. Time-synchronized cooperative jamming means that the radar would be simultaneously deceived by each jammer during the penetration process. Time-circulating cooperative jamming refers to the jamming mode in which the radar would be deceived by each jammer in turn, and the interference formed at the radar spans the entire jamming period. The jammer is turned on to deceive the radar when the protected target reaches the vicinity of the jammer.

It can therefore be seen that the analysis of the time-circulating cooperative jamming is similar to the

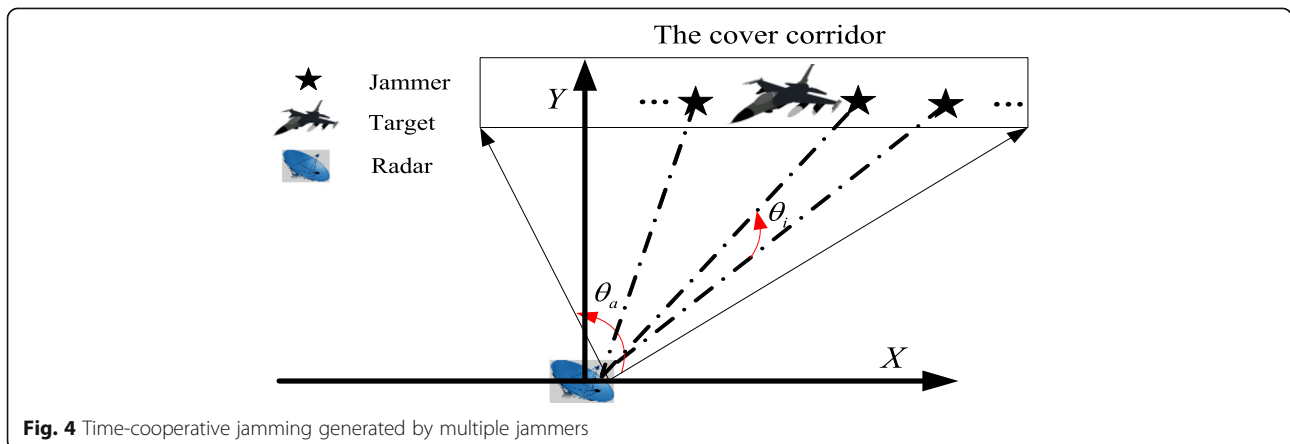


Fig. 4 Time-cooperative jamming generated by multiple jammers

power-cooperative jamming when the entire time-circulating cooperative jamming process is divided. Therefore, this paper mainly discusses selection of the jamming parameters and the radar's detection performance when using time-synchronized cooperative jamming.

Time-synchronized cooperative jamming generated by multiple jammers is shown in Fig. 4.

In Fig. 4, θ_a is the target's azimuth angle in the cover corridor. θ_i is the azimuth difference between the i th jammer and the $i + 1$ th jammer. The distance difference from the i th jammer to the $i + 1$ th jammer can be calculated as

$$S_{i,i+1} = \sqrt{R_i^2 + R_{i+1}^2 - 2R_iR_{i+1} \cos(\theta_i)} \tag{15}$$

where R_i and R_{i+1} are the distances from the i th and $i + 1$ th jammers to the radar, respectively. It is assumed that the radar's half-power beam width is $\theta_{i0.5}$ in order to ensure that at least one jammer exists in each of the radar's beam widths. That is, $\theta_i \leq \theta_{i0.5}$, the distance from the i th jammer to the $i + 1$ th jammer needs to be satisfied

$$S_{i,i+1} \leq S_{i,i+1(\max)} = \sqrt{R_i^2 + R_{i+1}^2 - 2R_iR_{i+1} \cos(\theta_{i0.5})} \tag{16}$$

When $\theta_i = \theta_{i0.5}$, the specific value of the jammer spacing mainly depends on the position and shape of the cover corridor.

Based on the azimuth angle, the expression of the jammers' number can be further deduced as

$$\text{num} = \text{ceil}\left(\frac{\theta_a}{\theta_i}\right) \geq \text{ceil}\left(\frac{\theta_a}{\theta_{i0.5}}\right) \tag{17}$$

4 Simulation results and discussion

4.1 Analysis of two detectors' detection in a homogeneous environment

According to (1), Table 2 lists the required scaling factor α to obtain $P_{FA, CA}$ and R as the parameters of the CA-CFAR.

According to (3) and (6), Fig. 5 lists the required scaling factor α when $R = 24$ for the OS-CFAR.

The behavior of the scaling factor α of the OS-CFAR detector is presented here as a function of K as shown in Fig. 5. The curves are parametric in the false alarm probability $P_{FA, OS}$. We can see that

Table 2 Scaling factor α for CA-CFAR with $P_{FA, CA}$ and R

$P_{FA, CA}$	$R = 8$	$R = 16$	$R = 24$	$R = 32$
10^{-4}	2.162	0.778	0.468	0.334
10^{-6}	4.623	1.371	0.778	0.540
10^{-8}	9.000	2.162	1.154	0.778

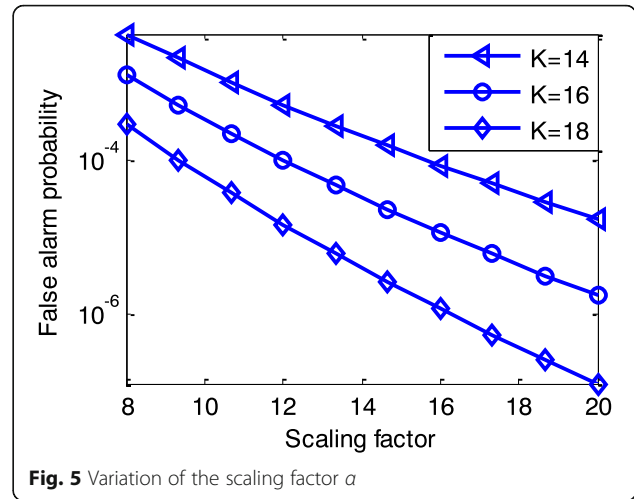


Fig. 5 Variation of the scaling factor α

the scaling factor α increases as $P_{FA, OS}$ decreases. The dip in the false alarm probability $P_{FA, OS}$ is caused by an increase in the scaling factor α and the parameter K .

In a homogeneous environment, according to (4)–(6), when the false alarm probability $P_{FA} = 10^{-6}$, $R = 24$. The performances of both CFAR systems are presented in Fig. 6 with different K and SNR values.

The detection characteristics of the OS-CFAR detector as a function of the primary target SNR, the rank of the cell ($K = 6, 12, 18$), and the results are shown in Fig. 6. For comparison, the CA-CFAR results are also shown in the same figure. Obviously, the CA-CFAR detector has the largest detection probability at any SNR censoring value. Thus, the CA-CFAR detector has better performance relative to the OS-CFAR detector when the noise background is homogeneous.

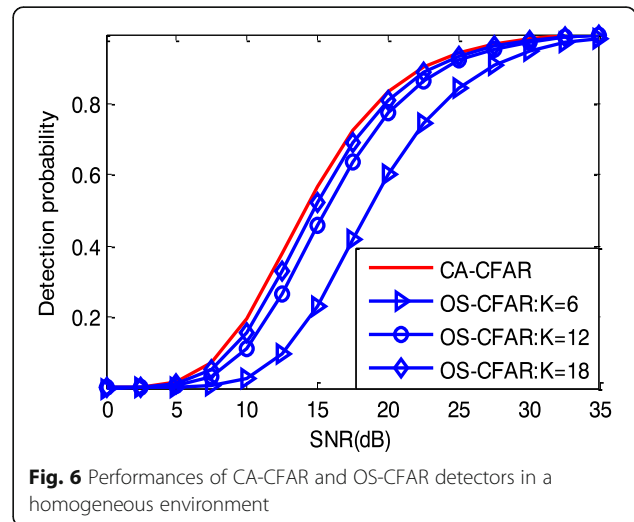
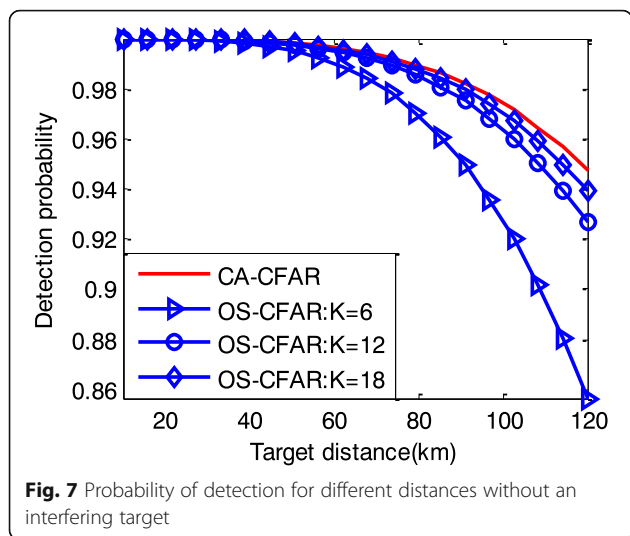


Fig. 6 Performances of CA-CFAR and OS-CFAR detectors in a homogeneous environment



4.2 Analysis of two detectors' detection in power-cooperative jamming

In this section, it is assumed that the enemy radar parameters have been accurately detected. The pulse compression radar's parameters in (11) are used, where $P_t = 1.5$ MW, $G_t = G_r = 30$ dB, $\lambda = 0.1$ m, $T = 50$ μ s, $B = 10$ MHz, $\sigma = 6$ m², $T_0 = 290$ K, $F = 3$ dB, and $L_t = 6$ dB.

It is assumed that the initial distance between the radar and the target $R_t = 120$ km and that the radar is interfered by two identical jammers. The two jammers arrive at the enemy radar with the target from far to near using the jammers' parameters in (12), where $G_j = 10$ dB, $L_j = 10$ dB, $\gamma_j = 10$ dB, and $P_j = 100$ W.

It is assumed that the number of the two detectors' reference cells $R = 24$, the length of the reference cell $L = 75$ m, the probability of a false alarm $P_{FA} = 10^{-6}$, and the rank of the representative cell in OS-CFAR $K = 3/4R = 18$.

In a homogeneous environment, Fig. 7 shows the detection probability of the two detectors as a function of distance with different K values.

In the following simulation, power-cooperative jamming would be generated by two jammers with the three interference modes in Table 1. The analysis of power-cooperative jamming will be divided into three cases. In the first case, the two jammers transmit noise frequency modulation power-cooperative jamming signals. In the second case, the two jammers transmit smart noise convolution power-cooperative jamming signals. In the third case, the two jammers transmit interrupted-sampling and periodic repeater power-cooperative jamming signals.

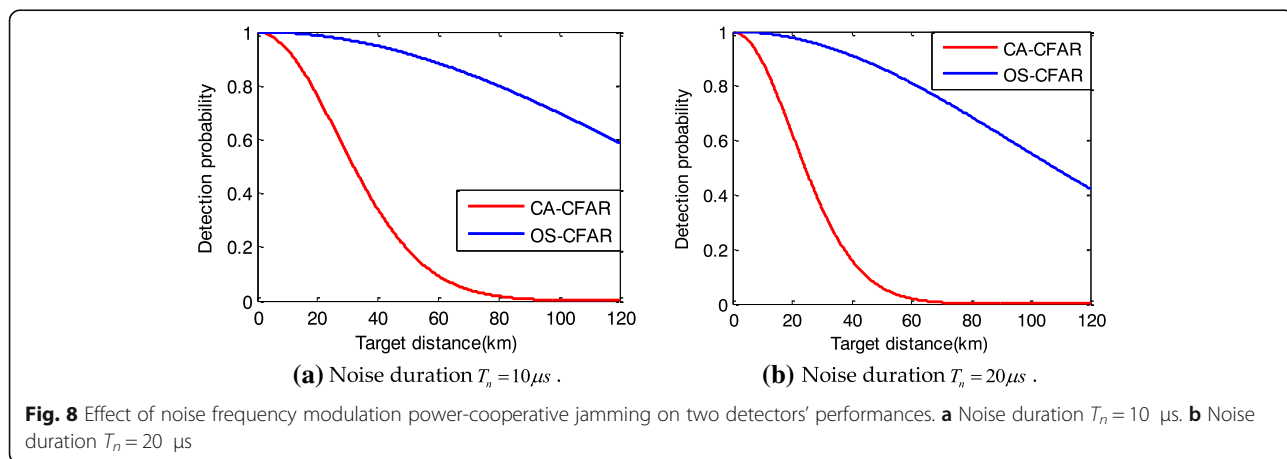
Case 1: Noise frequency modulation power-cooperative jamming

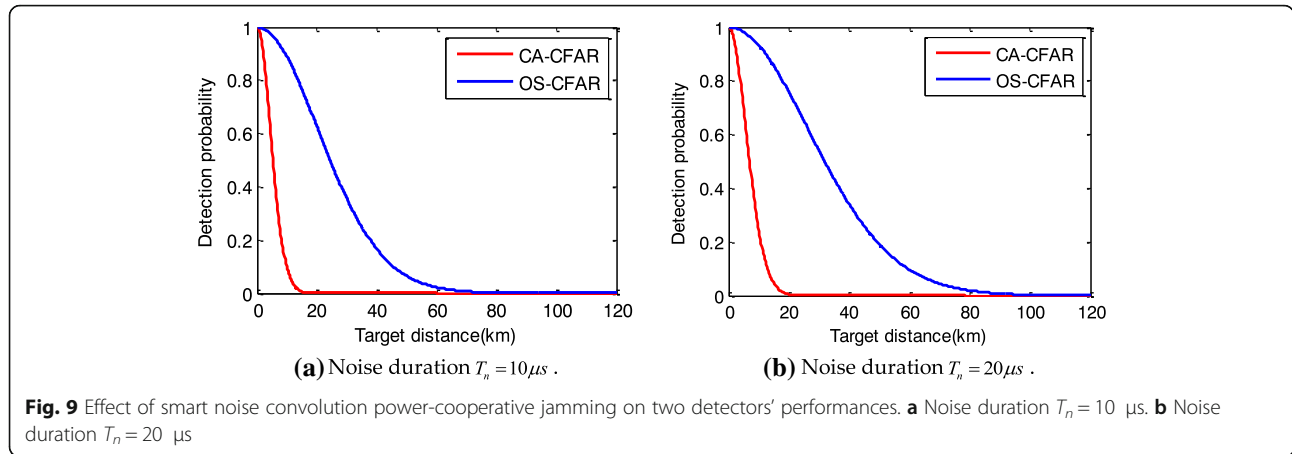
Figure 8 shows the detection probability at different distances with noise frequency modulation power-cooperative jamming for noise durations $T_n = 10$ μ s and $T_n = 20$ μ s. Comparing Fig. 8a and Fig. 8b with Fig. 7, it can be seen that the noise FM interference improves the detection threshold, and the detection probability of the two detectors on the target are both reduced. However, noise frequency modulation power-cooperative jamming cannot achieve a coherent processing gain by the pulse compression radar, and the probability of detection of the two detectors is still high. Therefore, it is necessary to increase the number of jammers and the jammers' power when simply implementing noise frequency modulation power-cooperative jamming.

Case 2: Smart noise convolution power-cooperative jamming

Smart noise convolution power-cooperative jamming has both noise jamming and coherent jamming characteristics. Comparing the simulation results from case 1 and case 2, the smart noise convolution power-cooperative jamming has a better interference effect than the noise frequency modulation power-cooperative jamming for the same noise duration.

From the theoretical analysis in Table 1, we know that the longer the noise duration of the smart noise convolution jamming is, the larger the barrage range of the





smart convolution jamming is to the radar, while the pulse compression gain is simultaneously reduced. The simulation results in Fig. 9a and Fig. 9b are consistent with the theoretical analysis.

Case 3: Interrupted-sampling and periodic repeater power-cooperative jamming

It is assumed that the sampling periods of the two jammers $T_s = 10 \mu s$, and the sampling time square τ and the repeater time T_r are each $1 \mu s$. There will be $M = 9$ independent main false targets, because $T_r > 2/B = 0.2 \mu s$. False target interval $\Delta d = c \cdot T_r / 2 = 150 \text{ m}$, i.e., $\Delta D = 1200 \text{ m}$ for the total false target distance, and $(R + 1)L = 25 \times 75 = 1875 \text{ m}$ in the total detector distance, which belongs to case 3 in Section 3.1. Assuming that the position error is large enough $\Delta r = 1200 \text{ m} > (R + 1)L - \Delta D + (M - 1 - (R - K))\Delta d$, the position error will affect the interference results of both detectors. At this time, two jammers are used for power coordination. According to (14), the maximum coverage of the false targets generated by the two jammers $\Delta D_{\max} = 2\Delta D = 2400 \text{ m}$.

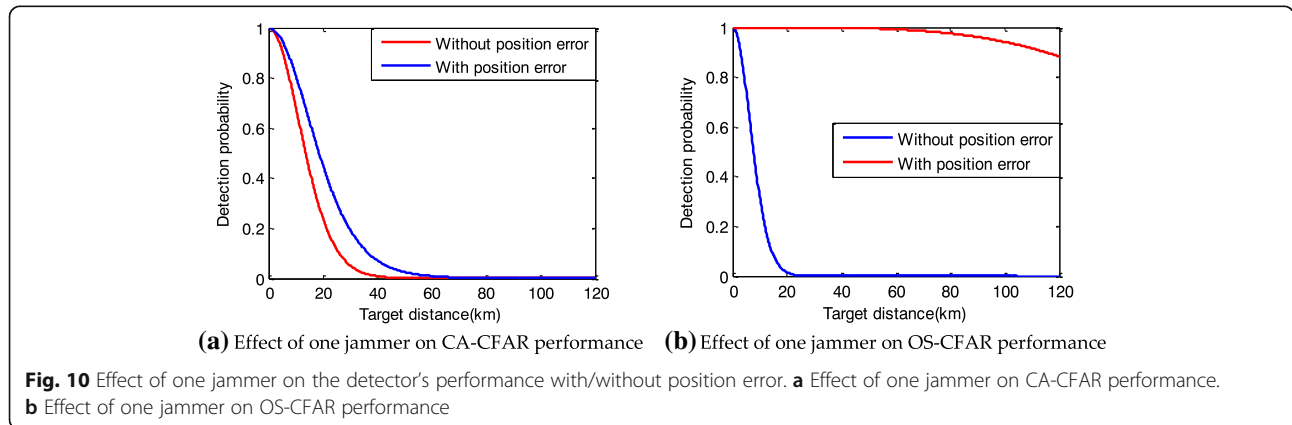
From the simulation results shown in Fig. 10a and Fig. 10b, it can be seen that the effect of one jammer on the two detectors' performances is inferior when there is an uncertain radar uncertain position. However, it has a greater impact on the OS-CFAR, because the number of false targets in the reference window is significantly less than $R - K$.

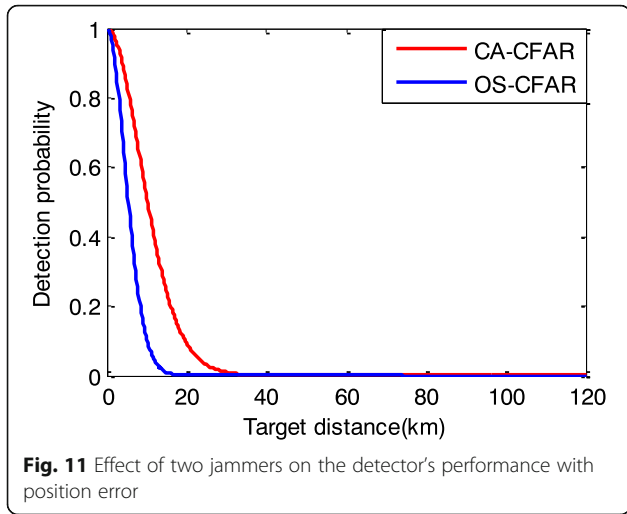
Two detectors' performance in the interfering targets generated by two jammers is shown in Fig. 11.

From the results in Fig. 11, it can be seen that the power coordination generated by two jammers can significantly reduce the detection probability of the two detectors. The number of false targets in the reference window is increased after interrupted-sampling and periodic repeater power-cooperative jamming is used, and the detection threshold is raised, which compensates for the influence of the radar uncertain position on the jamming.

4.3 Analysis of two detectors' detection for time-cooperative jamming

In this section, it is assumed that the target's azimuth angle in the cover corridor is $\theta_a = 90^\circ$, the radar half-power beam





width is $\theta_{i0.5} = 2^\circ$, the target's initial coordinates are (10 km, 17.32 km), the flying speed is $(-200 \text{ m/s}, 0 \text{ m/s})$, and the azimuth difference is $\theta_i = \theta_{i0.5} = 2^\circ$. To ensure that there is only one jammer in the main lobe during radar scanning, the number of jammers $\text{num} = 90/2 = 45$ and the jammers are evenly distributed in the cover corridor. Because the effect of time-cooperative jamming on the two detectors is similar, taking into account the length of the paper, the simulation only uses the detection results of the OS-CFAR detector for illustration.

The jammer and OS-CFAR detector parameters are the same as in Section 4.2, but the jamming power is different, set at 10 W and 100 W, respectively.

Comparing the simulation results in Fig. 12, it can be seen that time-cooperative jamming is an effective method on the OS-CFAR detector. When the azimuth angle is less than 60° , the detection probability increases because the target flies towards the enemy radar, and the distance from the target to radar decreases, while most of the jammers are located far from the target. When the azimuth angle

reaches 60° , the target is just at the center of the cover corridor. The gain of the radar antenna obtained by the jammer gradually reaches a maximum, and the detection probability of the OS-CFAR drops rapidly.

Figure 13 depicts the detection probability changes with different numbers of jammers: $\text{num} = 20$ and $\text{num} = 60$. When the number of jammers $\text{num} = 20$ is less than the design requirement in (17) of Section 3.2, the detection probability of the target will be less than 0.2 when flying in a short range in the center of the cover corridor.

Comparing Fig. 12a and Fig. 13b, it can be seen that an increase in the number of jammers does not significantly improve the jamming effect, and its greater role is to extend the length of the jamming cover corridor, which is shown in Fig. 14.

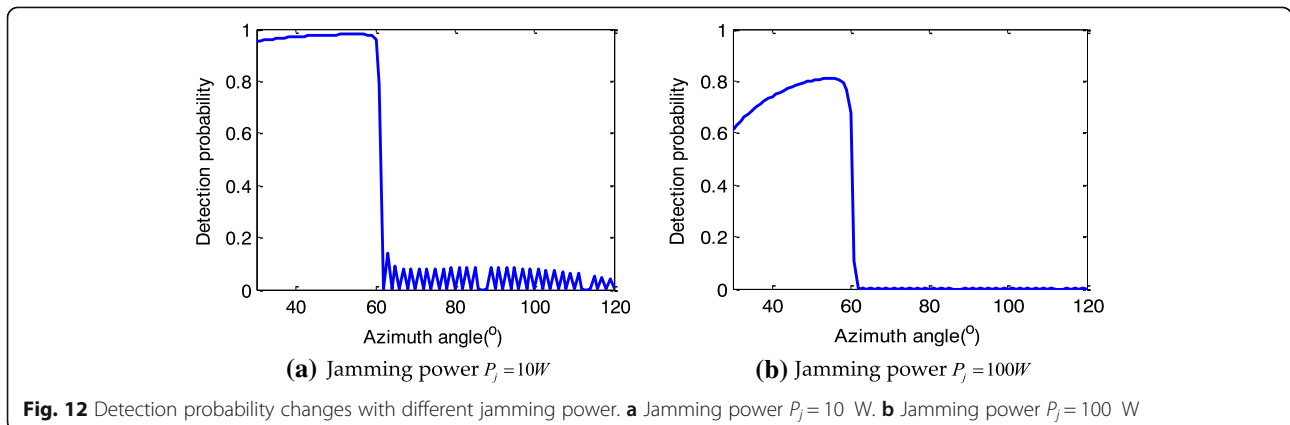
Based on the above analysis, in order to increase the length of the jamming cover corridor, the number of jammers should be increased. Specifically, if the length of the cover corridor is fixed, taking the cost into consideration, the number of jammers should be

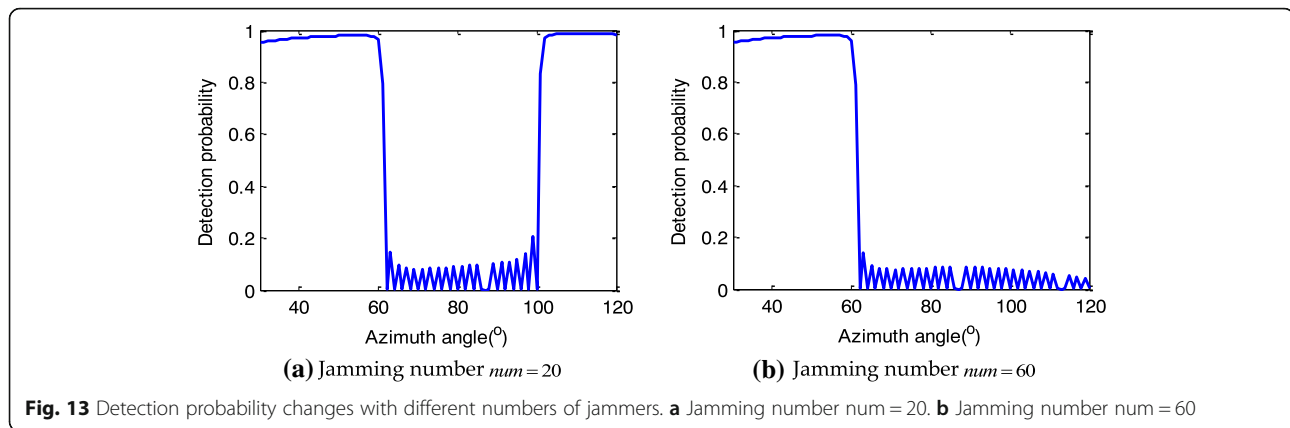
$$\text{num} = \text{ceil}(\theta_a / \theta_{i0.5}) \tag{18}$$

5 Conclusions

In this paper, two cooperative jamming methods are proposed for CFAR detectors without certain radar position information. First, several key parameters of the false targets are derived based on the principle of CFAR detection. Then, the influence of different jammer interference modes on the radar detection probability is analyzed in detail.

For power-cooperative jamming, noise frequency modulation and smart noise convolution power-cooperative jamming can more or less reduce the detection probabilities of CFAR detectors. Additionally, smart noise convolution power-cooperative jamming has a





better interference effect than noise frequency modulation power-cooperative jamming for the same noise duration. Interrupted-sampling and periodic repeater power-cooperative jamming can achieve a larger pulse compression gain than either of the two jamming methods mentioned above, but it is sensitive to the radar uncertain position. In summary, for power-cooperative jamming, noise barrage can be used to improve the noise floor and cooperate with deceptive jamming, i.e., interrupted-sampling and periodic repeater jamming, to accomplish power barrage.

With time-cooperative jamming, the number of jammers and their power can both influence the probabilities of CFAR detectors. The detection probabilities of the detectors both decrease as the number and power of jammers increase. When the target is just at the center of the cover corridor (the azimuth angle reaches 60° in the example shown in this paper), the detection probability of the detector drops rapidly. For time-cooperative jamming, the length of the cover corridor can be increased by increasing the number of jammers. If the length of the cover

corridor is fixed, in the interest of conserving resources, the number of jammers should be $\text{ceil}(\theta_a/\theta_{i0.5})$.

Our future work is to use cooperation jamming to deceive a radar's network. In particular, how to generate phantom tracks using a group of cooperating ECAVs should be considered, including the effect of radar position inaccuracies on the phantom track and the phantom track's cooperation and geometric constraints.

Abbreviations

CA-CFAR: Cell averaging constant false alarm ratio; CFAR: Constant false alarm ratio; DRFM: Digital radio frequency memory; INR: Interference-to-noise ratio; LFM: Linear frequency modulation; ML-CFAR: Mean level constant false alarm ratio; OS-CFAR: Orderly statistics constant false alarm ratio; RCS: Radar cross section; SNR: Signal-to-noise ratio

Acknowledgements

The authors want to acknowledge the help of all the people who influenced the paper. Specifically, they want to acknowledge the editor and anonymous reviewers for their valuable comments.

Funding

There is no source of funding for this paper.

Availability of data and materials

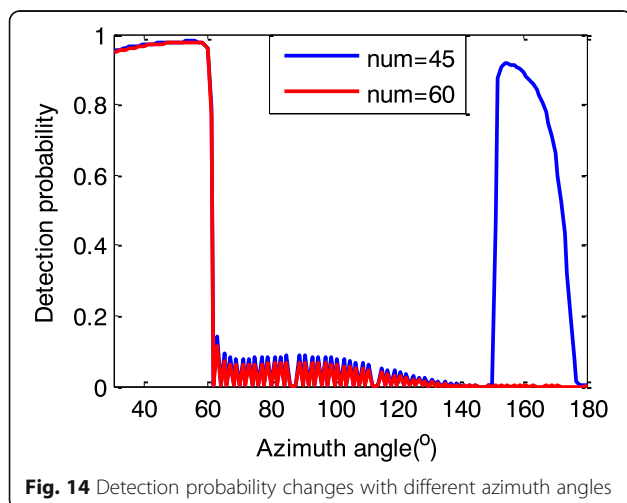
Data sharing is not applicable to this article as no datasets were generated or analyzed during the current study.

Results and discussion section

Section 4 of the manuscript—Simulation results and discussion—can be seen as the combination of the results section and the discussion section.

Methods/experimental section

In this work, one important issue in radar jamming is the effect of inaccuracies in radar position, which leads to a greatly reduced number of false targets entering the reference window of the constant false alarm ratio (CFAR) detector. Therefore, two cooperative jamming methods specifically for the pulse compression radar with CFAR detector are proposed in this paper. We used MATLAB software on a computer to generate simulation data for experimenting according to the radar parameters described in the manuscript. We applied the proposed algorithm to the simulation data and analyzed the corresponding results. The theoretical analysis and computer simulation justify the methods' validity and efficiency. The obtained conclusion has a certain guiding significance for the practical application of jamming against pulse compression radar.



Authors' contributions

XL is the primary author of this paper, who developed the simulations and wrote the first draft of the paper. DSL scientifically supervised the work and acted as his academic advisor through the duration, providing feedback at all levels. Both authors read and approved the final manuscript.

Ethics approval and consent to participate

Not applicable.

Competing interests

The authors declare that they have no competing interests.

Publisher's Note

Springer Nature remains neutral with regard to jurisdictional claims in published maps and institutional affiliations.

Received: 26 April 2018 Accepted: 25 October 2018

Published online: 06 November 2018

References

1. M.A. Richards, *Fundamentals of Radar Signal Processing* (McGraw-Hill Professional Publishing, New York, 2005)
2. H. You, G. Jian, M.X. Wei, *Radar Target Detection and CFAR Processing* (Tsinghua University Press, Beijing, 2011)
3. Z. Messali, F. Soltani, Performance of distributed CFAR processors in Pearson distributed clutter. *EURASIP J. Adv. Signal. Process.* **2007**, 1–7 (2007)
4. N. Janatian, M.M. Hashemi, A. Sheikhi, CFAR detectors for MIMO radars. *Circuits Syst. Signal Process* **32**(3), 1389–1418 (2013)
5. L. Kong, B. Wang, G. Cui, W. Yi, X. Yang, Performance prediction of OS-CFAR for generalized sterling-chi fluctuating targets. *IEEE Trans. on Aerospace and Electronic Systems* **52**(1), 492–500 (2016)
6. S. Blake, OS-CFAR theory for multiple targets and nonuniform clutter. *IEEE Trans. on Aerospace and Electronic Systems* **24**(6), 785–790 (1988)
7. D.J. Feng, Y. Yang, L.T. Xu, Impact analysis of CFAR detection for active decoy using interrupted-sampling repeater. *J. China Univ. Defense Technol.* **38**(1), 63–68 (2016)
8. M.X. Fang, J.G. Wang, Y.J. Yang, Evaluation on netted radar detection performance in the distributed jamming of multi-false target. *Mod. Def. Technol.* **42**(3), 135–141 (2014)
9. L.F. Shi, Y. Zhou, D. Li, Multi-false-target jamming effects on the LFM pulsed radar's CFAR detection. *J. Syst. Eng. Electron.* **27**(5), 818–822 (2005)
10. Y R Zhang, M G Gao, Y J Li, In Proceedings of 2014 IEEE 9th Conference on Industrial Electronic and Application (ICIEA). Performance Analysis of the Mean Level CFAR Detector in the Interfering Target Background IEEE, (2014), pp.1045–1048
11. W. X S, L. J C, W.M. Zhang, Mathematic principles of interrupted-sampling repeater jamming. *Sci. China Ser. F Inform. Sci.* **50**(1), 113–123 (2007)
12. Z. S S, Z. L R, Discrimination of active false targets in multistatic radar using spatial scattering properties. *IET Radar, Sonar & Navig* **10**(5), 816–826 (2016)
13. K. Chaisoon, DARPA issues wolfpack solicitation. *J. Electron. Def.* **24**(5), 16 (2001)
14. K. J, DARPA moves forward on plan to develop swarms of cooperating drones. *Military & Aerospace Electronics* **27**(5), 4–6 (2016)
15. K. J, DARPA to develop swarming unmanned vehicles for better military reconnaissance. *Military & Aerospace Electronics* **28**(2), 4–6 (2017)
16. R. Scott, Unmanned upstart: Kratos casts off its cloak. *Jane's International Defense Review* **49**, 36–39 (2016)
17. M. Pachter, P.R. Chandler, R.A. Larson, K.B. Purvis, *Proceedings of AIAA Guidance, Navigation, and Control Conference and Exhibit. Concepts for Generating Coherent Radar Phantom Tracks Using Cooperating Vehicles AIAA* (2004), pp. 1–14
18. B.P. Keith, P.R. Chandler, M. Pachter, Feasible flight paths for cooperative generation of a phantom radar track. *J. Guid. Control Dynam.* **29**(3), 653–661 (2006)
19. I.I.H. Lee, H.A. Bang, A cooperative line-of-sight guidance law for a three-dimensional phantom track generation using unmanned aerial vehicles. *J. Aerosp. Eng.* **227**(6), 897–915 (2016)
20. L. Y A, N. T Q, et al., Application of simulated annealing algorithm in optimizing allocation of radar jamming resources. *Syst. Eng. Electron.* **31**(8), 1914–1300 (2009)
21. X M Li, T L Dong, G M Huang, Distribution method of jamming power to radar net based on two-person zero-sum game. *J. Sichuan Univ.*, 48(3), 129–135 (2016)
22. Z. Y R, G. M G, L. H Y, L. Y J, Evaluation method of cooperative jamming effect on radar net based on detection probability. *J. Syst. Eng. Electron.* **37**, 1778–1786 (2015)
23. M. Pachter, P.R. Chandler, R.A. Larson, K.B. Purvis, in *Concepts for Generating Coherent Radar Phantom Tracks Using Cooperating Vehicles AIAA. Proc. AIAA guidance, navigation, and control conference and exhibit, providence* (2004), pp. 1–14
24. N. Dhananjay, D. Ghose, Generation of a class of proportional navigation guided interceptor phantom tracks. *J. Guid. Control Dynam.* **38**(11), 2206–2214 (2015)
25. N. Levanon, Detection loss due to interfering targets in ordered statistics CFAR. *IEEE Trans. Aerosp. Electron. Syst.* **24**(6), 678–681 (1988)
26. Z. Y R, L. Y G, G. M G, Optimal assignment model and solution of cooperative jamming resources. *J. Syst. Eng. Electron.* **36**(9), 1744–1749 (2014)
27. D.C. Schleher, *Electronic Warfare in the Information Age* (Artech House, Norwood, 1999)

Submit your manuscript to a SpringerOpen[®] journal and benefit from:

- Convenient online submission
- Rigorous peer review
- Open access: articles freely available online
- High visibility within the field
- Retaining the copyright to your article

Submit your next manuscript at ► springeropen.com